

1 **How the spontaneous perception of face pareidolia unfolds over time**

2

3 Amanda K Robinson^{1,2,3}, Greta Stuart¹, Sophia M Shatek^{3,4}, Adrian Herbert¹, Jessica Taubert^{1*}

4

5 ¹School of Psychology, The University of Queensland, Australia.

6 ²Queensland Brain Institute, The University of Queensland, Australia.

7 ³School of Psychology, University of Sydney, Australia.

8 ⁴Department of Experimental Psychology, University of Oxford, UK.

9

10 * Corresponding author. j.taubert@uq.edu.au

11

12 **Funding:**

13 Australian Research Council Discovery Early Career Researcher Award DE200101159 (AKR).

14 Australian Research Council Future Fellowship FT200100843 (JT).

15

16 **Competing interests:** Authors declare that they have no competing interests.

17

18 **Data and materials availability:** All code, stimuli and behavioral data will be available upon
19 publication.

20

21 **Abstract**

22

23 The human brain rapidly detects faces, even in inanimate objects—a phenomenon known as face
24 pareidolia. While this illusion reveals the automaticity of face detection, it also presents a paradox: how
25 does the brain process stimuli that are simultaneously faces and objects? Here, we combined behavioral
26 experiments with electroencephalography to track the temporal dynamics of face pareidolia processing.
27 Using a large stimulus set of human faces, objects containing illusory faces, and matched control objects,
28 we show that perception of face pareidolia is remarkably flexible and task dependent. When making
29 spontaneous similarity judgments, participants perceived illusory faces as intermediate between faces
30 and objects. However, in explicit categorization tasks, the same stimuli were predominantly classified as
31 objects, while rating face-likeness bolstered the representation of face-like features. Neural responses
32 tracked this perceptual flexibility: early visual processing (90-130ms) correlated with face-like
33 judgments, while later activity (150-210ms) aligned with object categorization. This temporal progression
34 demonstrates how the brain maintains multiple levels of representation, integrating early face detection
35 with subsequent object recognition to support flexible behavior. Our findings demonstrate that face
36 pareidolia exemplifies the brain's capacity to resolve perceptual ambiguity through dynamic processing,
37 with task demands determining how competing representations contribute to perception.

38 The primate brain responds differently to faces and objects. This ubiquitous finding, which transcends all
39 recording (Dy et al., 2006; Quian Quiroga et al., 2023; Taubert et al., 2015), imaging (Kanwisher et al.,
40 1997; Puce et al., 1996; Rossion et al., 2012; Taubert et al., 2022), and causal (Afraz et al., 2006; Azadi
41 et al., 2023; Sadagopan et al., 2017) methods, has led to an unresolved debate: do faces engage distinct
42 neural mechanisms, separate from those processing objects (Kanwisher, 2000)? Or, alternatively, do
43 visually evoked responses reflect a distributed code that can universally classify any visual stimulus as a
44 function of image properties (Kriegeskorte et al., 2008)? These questions, while central to our
45 understanding of primate vision and brain topography, have been largely rendered intractable, in part
46 because it is difficult to decouple a face from the image properties that typically define a face. Difficult
47 but not impossible.

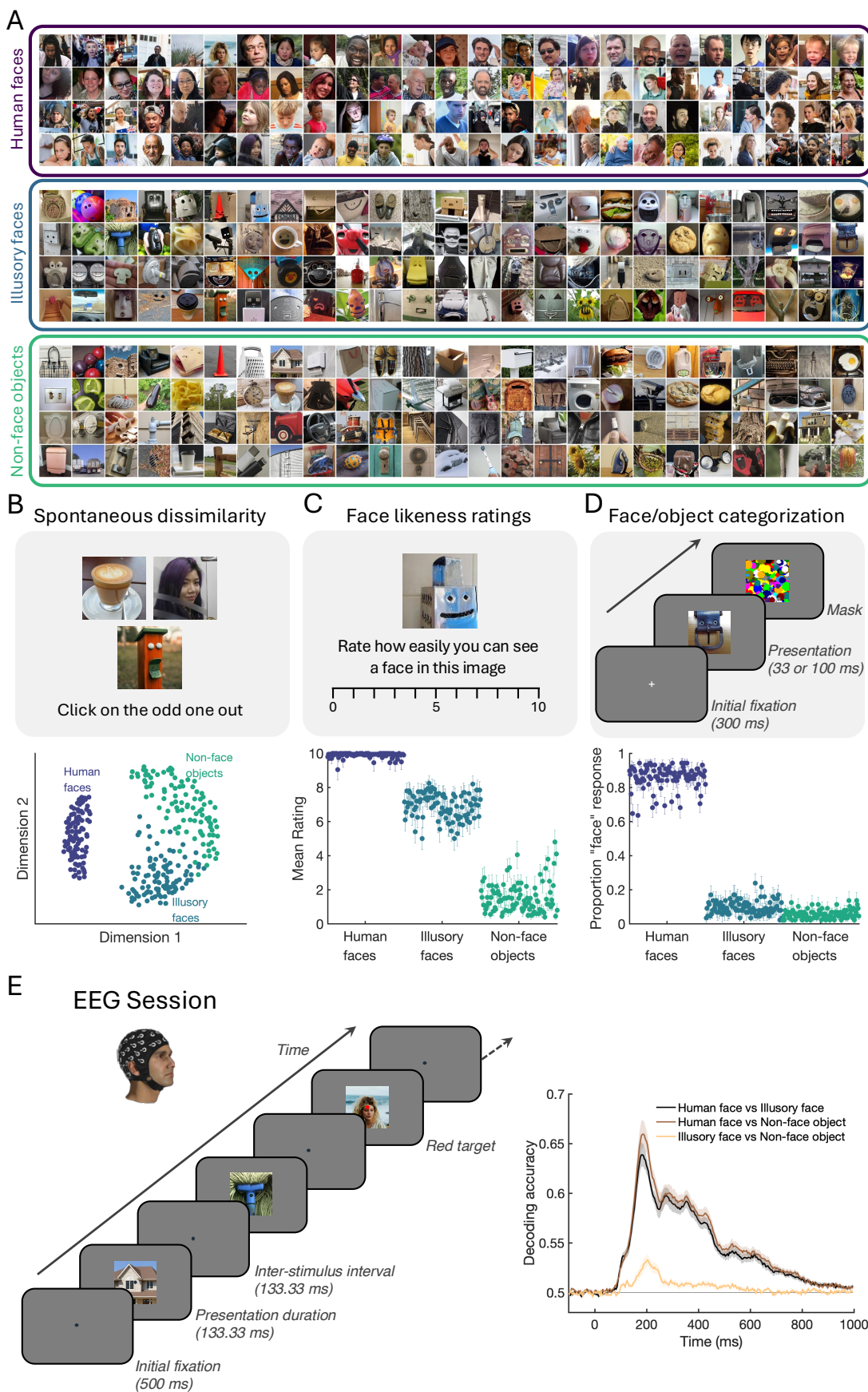
48 Face pareidolia is the common experience of perceiving a face in an otherwise inanimate object
49 (Meng et al., 2012; Omer et al., 2019; Taubert et al., 2017). Interestingly, while these stimuli are easily
50 perceived as face-like, their image properties are more typical of inanimate objects (Epikhova et al., 2022;
51 Keys et al., 2021; Sairels et al., 2024). Thus, examples of face pareidolia provide a rare opportunity to
52 understand how image properties contribute to the neural representation of faces and objects. For
53 instance, examples of face pareidolia have been used to show that the brain's response to a visual
54 stimulus evolves over time (Decramer et al., 2021; Rekow et al., 2022; Wardle et al., 2020); patterns of
55 brain activity first encode examples of face pareidolia as being more similar to faces, and then more
56 similar to objects (Wardle et al., 2020). This is consistent with a system that has distinct mechanisms
57 underscoring distinct, potentially parallel, functions. To date, however, there is no evidence that the
58 evolving neural signature of face pareidolia has behavioral consequences. In other words, when we
59 experience the face pareidolia illusion, do we first see a face and then an object?

60 Studies of face pareidolia at the behavioral level have been narrowly focused on the perception
61 of illusory faces, often asking participants to rate how face-like an image is on an ordinal scale (Taubert
62 et al., 2023; Wardle et al., 2020, 2022) or to locate face-like patterns in natural scenes (Meng et al., 2012;
63 Uchiyama et al., 2012) or pure noise (Liu et al., 2014). These tasks motivate participants to actively
64 search for evidence of face-like features, potentially biasing behavior. Further, these responses correlate
65 with brain activity late in the time course (see Romagnano et al., 2024; Wardle et al., 2020), suggesting
66 that they index cognitive decisions rather than early sensory processes or spontaneous behaviors that
67 occur without awareness. What is needed are better behavioral markers of the face pareidolia illusion,
68 where participants are not instructed to search for, or evaluate, facial attributes.

69 To address this knowledge gap, we used an odd-one-out triplet task to measure perceived
70 dissimilarity among a large number of images comprised of 100 human faces, 100 objects with illusory
71 facial features (hereafter referred to as illusory faces) and 100 matched objects (Figure 1A,B). This task
72 has been used to characterize the latent featural dimensions underlying visual recognition, without
73 constraining or guiding participant responses (Grootswagers et al., 2024; Hebart et al., 2020). Assuming
74 the face pareidolia illusion is perceived spontaneously, even when participants are not instructed to look
75 for faces, we predicted that illusory faces would be perceived as more similar to each other than to their
76 non-face objects counterparts, despite being matched for semantic content. Additionally, for all 300
77 stimuli, we collected face-like ratings, predicting that the ratings given to illusory faces in this behavioral
78 context would better reflect their illusory face identity (Figure 1C), and responses during a face-object
79 categorization task, predicting that responses to illusory faces in this behavioral context would better
80 reflect their veridical object identity (Figure 1D). Then we collected time-resolved visual evoked
81 responses to the 300 stimuli using EEG (Figure 1E). Our goal was to properly contextualize human
82 behavior towards examples of face pareidolia, relative to both real faces and ordinary objects, and then
83 leverage those observations to better understand how the evolving neural representation of face
84 pareidolia supports behavioral responses.

85 We discovered that behaviors capturing the illusory face identity in examples of face pareidolia
86 correlate with brain activity at an earlier time point than behaviors that only capture the veridical object
87 identity in examples of face pareidolia. Additionally, behavior in the odd-one-out triplet task discriminated
88 between nested pairs of visual stimuli (i.e., illusory face and matched object pairs that belong to the same
89 semantic category) at earlier stages of processing than performance in the speeded categorization.
90 Collectively, these powerful observations suggest that the mechanisms responsible for detecting faces,
91 i.e., distinguishing real and illusory faces from other kinds of visual stimuli, are distinct from those
92 responsible for recognizing objects. First, the visual system rapidly detects face-like features based on
93 the image properties that illusory faces share with real human faces. Subsequently, it processes the
94 object's true identity (such as vegetable or car) by analyzing the image properties that illusory faces share
95 with objects.

96

Figure 1. Experimental design.

99 Note. (A) Stimuli were 300 images of human faces, illusory faces in objects and matched non-face objects, used for three
100 different behavioral tasks and the EEG session. (B-D) Behavioral tasks and results. (B) Triplet odd-one-out task, capturing
101 spontaneous dissimilarity judgements across images in the stimulus set. Multi-dimensional scaling of the dissimilarity scores
102 revealed three clusters for the categories of human faces, illusory faces and objects. (C) Face-like ratings task. Participants
103 were asked to give a face-like rating to each stimulus on a scale from 0-10. Illusory faces were rated in between objects and
104 human faces. (D) Categorization task. In each trial, participants were presented with a stimulus that was backward masked
105 and asked to categorize it as a face or object. Results revealed illusory faces were largely judged as objects. (E) Example
106 sequence timeline from EEG experiment (left) and results from decoding the three categories (right). Participants viewed
107 sequences of stimuli at 3.75 Hz while their neural responses were measured with EEG. Throughout the session, they
108 performed an orthogonal fixation color change detection task. Mean decoding accuracy is shown for category pairs over time,
109 compared to chance (50%), showing a similar pattern of results to previous work (Wardle et al., 2022).

110

111 **Results**

112 *113 Behavioral tasks reveal context-dependent processing of illusory faces*

114 Our investigation into the neural processing of illusory faces for visual recognition employed three
115 complementary behavioral tasks, each probing different aspects of behavioral recognition; (1) perceptual
116 similarity, (2) face-like appearance and (3), face-object categorization. To this end, separate groups of
117 participants performed tasks of spontaneous dissimilarity judgments ($N = 338$), explicit face-likeness
118 ratings ($N = 20$), and speeded face-object categorization ($N = 23$) based on the same 300 stimuli. These
119 results unveiled a remarkable flexibility in how the human visual system builds multiplexed
120 representations of illusory faces.

121

122 First, in the spontaneous dissimilarity task, participants performed odd-one-out judgments among
123 triplets of stimuli (Figure 1B). As predicted, the resulting multidimensional similarity space revealed a
124 striking organization: while human faces and non-face objects formed distinct clusters, illusory faces fell
125 midway between them. Although the illusory faces were positioned closer to the object cluster than the
126 face cluster, there was little overlap between the illusory faces and matched objects. This organization
127 suggests that illusory faces have an inherent dual nature (Saurels et al., 2024; Stuart et al., 2025) and are
128 spontaneously perceived as distinct from ordinary objects even when participants are not prompted to
129 look for face-like features.

131 Next, the face-likeness rating task captured a different aspect of the graded nature of illusory face
132 perception. Importantly, human faces garnered near-ceiling face-like ratings ($M = 9.90$, $SE = .02$), while
133 non-face objects received minimal face-like scores ($M = 1.54$, $SE = .09$) indicating that participants
134 understood the task and aligning these results with previous studies (Taubert et al., 2023; Wardle et al.,
135 2020, 2022). Interestingly, illusory faces elicited robust face-like ratings ($M = 6.93$, $SE = .07$) that were
136 significantly lower than human faces ($t_{19} = -7.03$, $p < .001$) but also significantly higher than objects ($t_{19} =$
137 13.14 , $p < .001$). The observation that the mean face-like ratings for illusory faces were above 5 ($t_{19} = 4.30$,
138 $p < .001$) reflects a bias towards rating illusory faces as being more face-like than object-like. This bias is
139 consistent with previous studies using this approach (Taubert et al., 2023; Wardle et al., 2020, 2022) and
140 confirms the perception of facial features in this large set of illusory face stimuli.

141

142 Finally, the speeded categorization task revealed a different behavioral response profile. When forced to
143 make binary face-object decisions, participants predominantly classified illusory faces as objects
144 (proportion face response $M = .10$, $SE = .03$). This rate was dramatically lower than for human faces ($M =$
145 $.86$, $SE = .02$; $t_{21} = -20.77$, $p < .001$) and only marginally higher than for non-face objects ($M = .06$, $SE =$
146 $.01$; $t_{21} = 1.91$, $p = .070$). These findings suggest that when instructed to make categorical decisions, the
147 veridical object identity takes precedence over illusory facial characteristics and illusory faces are
148 reported as being mere objects. In sum, by employing the same stimuli over three independent behavioral
149 tasks, each time collecting a new sample of participants, we show that the behavioral context changes
150 how participants respond to face pareidolia. On the one hand, certain tasks will capture, and even
151 augment, the face-like appearance of the illusory identity, while on the other hand, other tasks will unbind
152 and ignore the illusory identity in favor of the true, veridical identity. Importantly, when we measured
153 perceptual similarity using the triplet odd-one-out task, we confirmed that when unprompted by
154 instruction and unconstrained by time participants spontaneously perceived illusory faces in examples
155 of face pareidolia and reported them as being distinct from matched non-face objects.

156

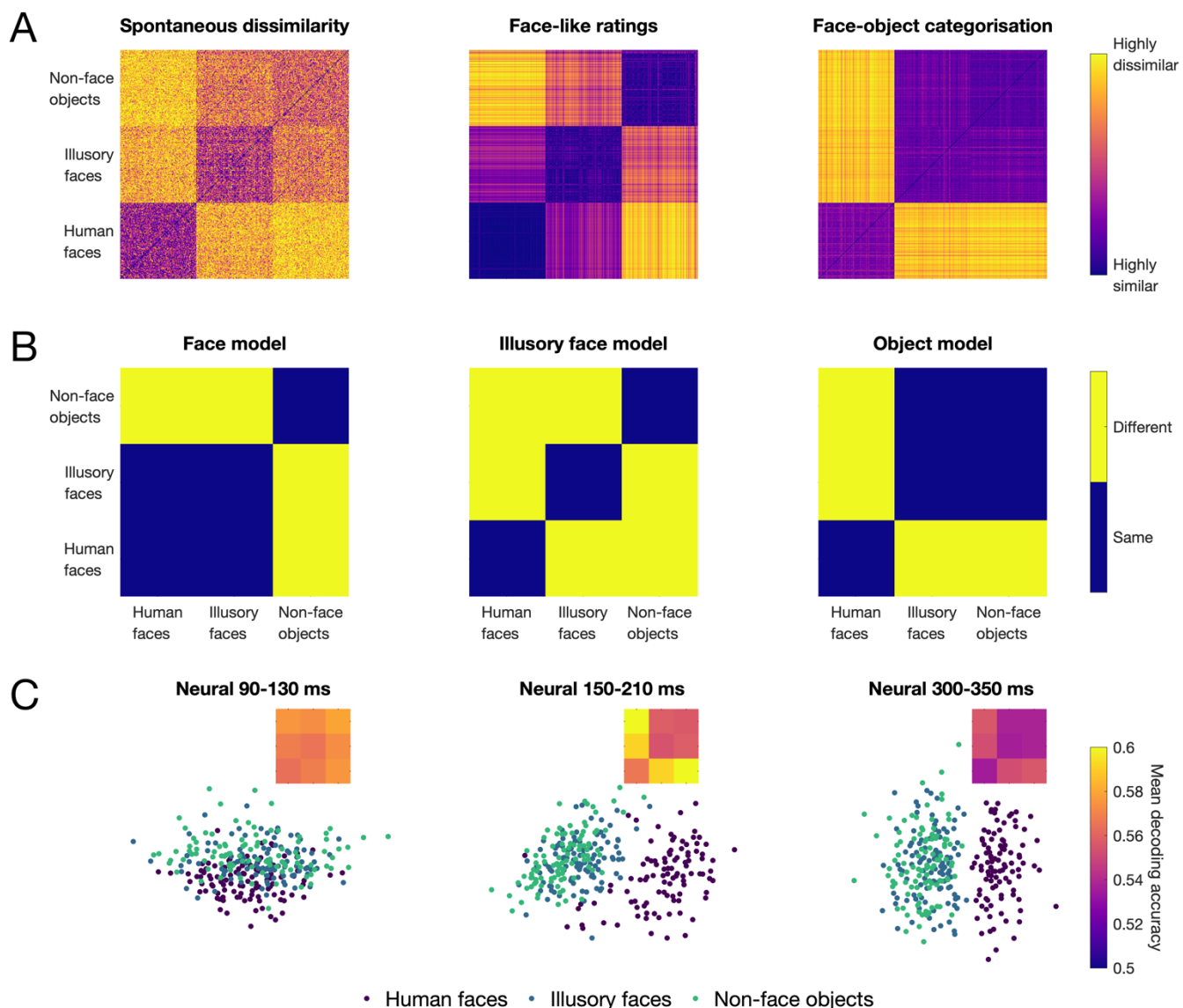
157 *Neural dynamics track behavioral flexibility*

158 Having established that perceived identity of illusory faces is malleable, our key question is whether these
159 different identities are represented at different stages of neural processing. To bridge neural processing
160 with behavior, we employed representational similarity analysis (RSA) to map the dynamics of stimulus

161 processing. Representational dissimilarity matrices (RDMs) were constructed for the neural
162 representations at each time point, each behavioral task, and three category models (Figure 2), and then
163 the neural RDMs were correlated with each task and category RDM. This approach revealed rich temporal
164 patterns linking neural representations to behavioral judgments across our tasks (Figure 3A).

165

166 **Figure 2. Representations of human faces, illusory faces and objects in behavior, categories and**
167 **neural responses.**



168 Note. A) Representational dissimilarity matrices (RDMs) based on behavior from the spontaneous dissimilarity, face-like and

169 categorization tasks. B) Face-object category models that vary according to the category assigned by illusory
170 faces are coded equivalent to human faces (face model), coded as a separate third category (illusory face model), and coded
171 equivalent to objects (object model). C) Neural representations of the 300 experimental stimuli from three different stages of
172

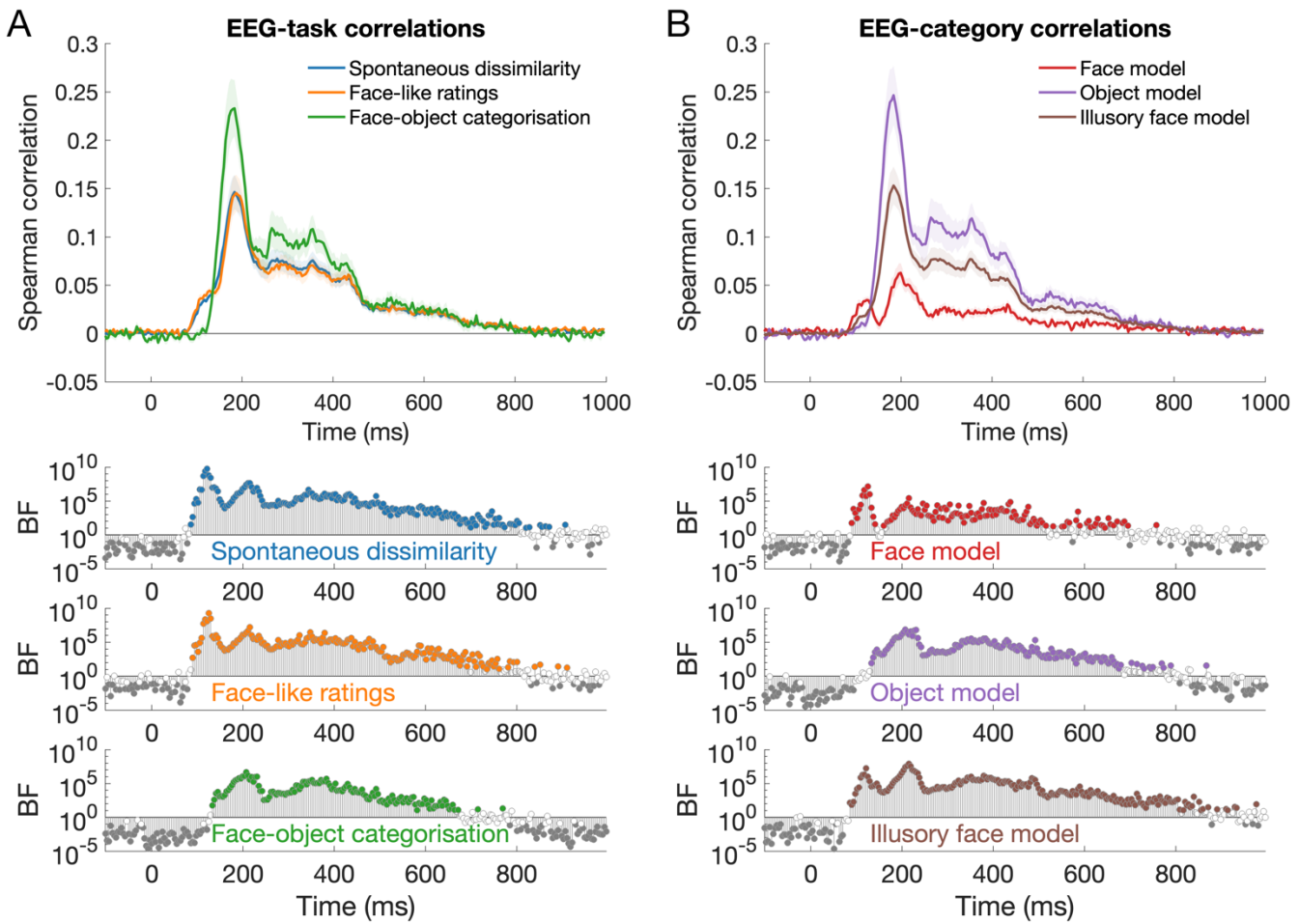
173 processing using multi-dimensional scaling. Inset plots show mean neural decoding RDMs from that time period,
174 downsampled to the category level.

175

176 The earliest neural processing stage (90-130 ms) showed reliable correlations with spontaneous
177 dissimilarity judgments and face-likeness ratings, but notably not with categorical face-object decisions
178 (Figure 3A). This early window appears to capture initial face-like processing of illusory stimuli, as
179 confirmed by stronger correlations with a face-based category model compared to an object-based
180 model (Figure 3B). However, a dramatic shift occurred in the 150 -210 ms window; neural patterns
181 showed the strongest correlation with face-object categorization behavior (Figure 3A) and the object-
182 based category model (Figure 3B). This temporal transition indicates that a rapid re-coding of illusory
183 faces takes place, shifting from an initial face-like representation to strict object representation. In the
184 third distinct time window (300-350ms), the neural information patterns again favored face-object
185 categorization over spontaneous dissimilarity judgements and face-like scores, but with lower fidelity
186 than during the second time window. This persistence of object-like categorical processing, rather than
187 a return to perceptual similarity, suggests that the brain maintains and refines canonical category
188 representations even in late processing stages. Overall, this evolving neural signature helps explain the
189 flexibility in human behavior in regard to face pareidolia; when we see an example of face pareidolia, the
190 brain is equipped to build and maintain multiplexed representation of that stimulus.

191

Figure 3. Neural representations of illusory faces and their behavioral relevance.



192

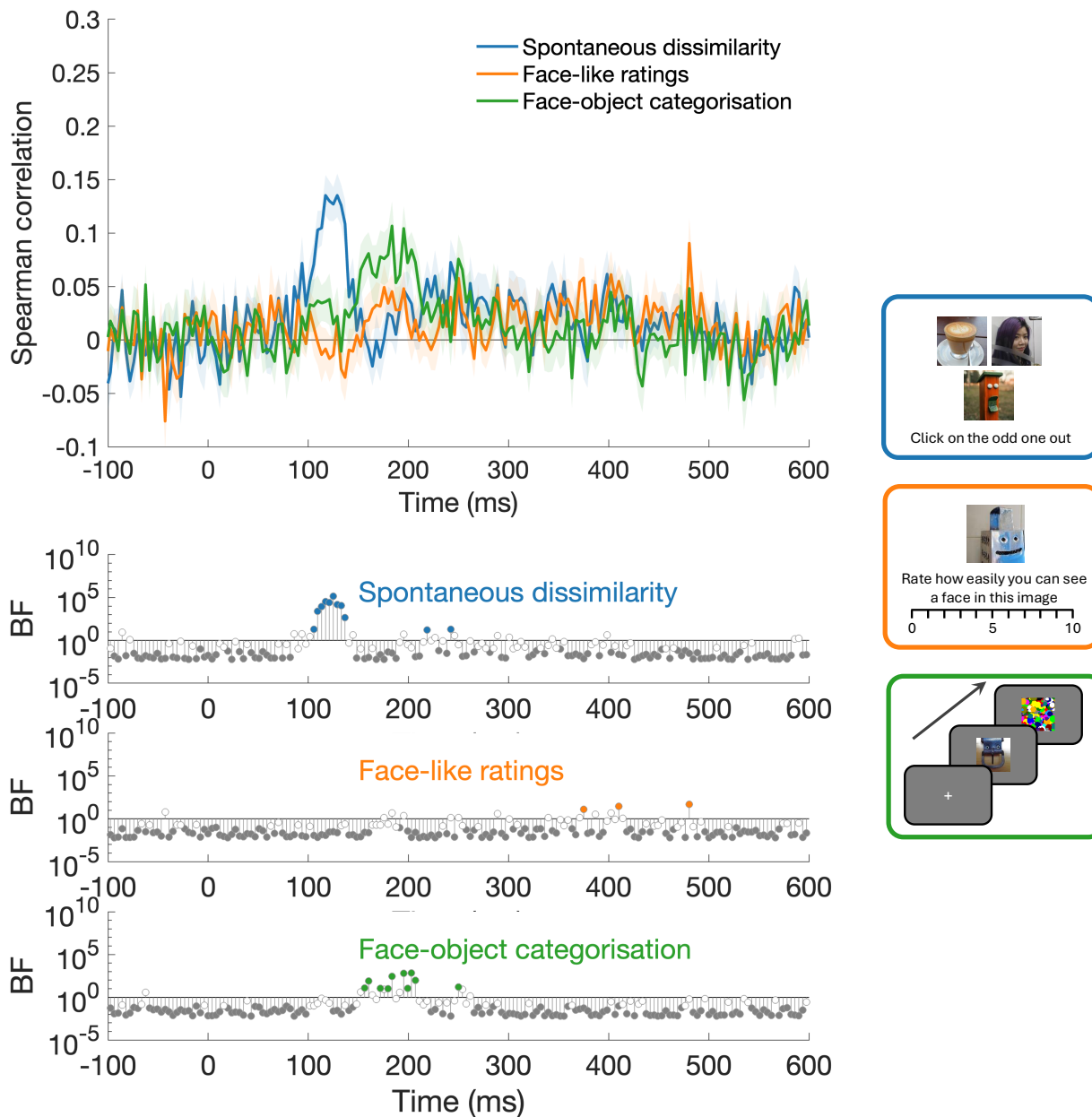
193 Note. Time-varying correlations between neural responses, behavior and visual category models. (A) Responses on three
 194 different behavioral tasks reflected different dynamics in the neural signal. (B) Category models that considered illusory faces
 195 either equivalent to human faces, equivalent to objects, or a distinct third category, correlated differentially with neural
 196 representations over time. Specifically, the face model had the highest correlation for the first stage of processing but was
 197 rapidly overtaken by the object model. These results indicate a change in illusory face processing over time, where illusory
 198 faces initially and briefly resemble human faces but subsequently resemble objects.

199

200

201 *Faces in objects: behavior reflects multidimensional brain responses*

202 Beyond larger categorical distinctions, we refined our analysis to examine the 100 pairs of nested stimuli
203 included in the design. Each pair was comprised of an illusory face and a matched non-face object (e.g.,
204 a cookie with an illusory face and a cookie without an illusory face). Figure 4 shows the neural-behavior
205 correlations for the nested pairs across the three tasks. The neural dissimilarity between stimulus pairs
206 correlated with spontaneous dissimilarity judgments during early processing (105-136 ms, BF_s > 20),
207 whereas the face-likeness ratings showed no reliable correlation, and the face-object categorization task
208 exhibited a neural-behavioral relationship that was later in the time course (156 – 207 ms, BF_s > .55,
209 median BF = 10.55). This temporal dissociation provides further evidence that tasks yield different
210 insights into image separability in the brain. Notably, the spontaneous triplet task proved particularly
211 valuable by capturing multiple levels of image dissimilarity (i.e., category-level and exemplar-level)
212 without explicit instruction, demonstrating its effectiveness as a measure of natural visual processing.

Figure 4. Neural representations of illusory faces and their behavioral relevance.

215 Note. Time-varying correlations between neural responses and behavioral tasks for the 100 nested stimulus pairs,
 216 consisting of illusory faces and matching non-face objects. Neural information was correlated with responses on the
 217 spontaneous dissimilarity task (blue) from early stages of processing, and the face-object categorization task (green) later in
 218 the time course. No consistent reliable correlation was captured for the face-like ratings (orange).

219 **Discussion**

220 *Behavioral Flexibility and Task Dependencies*

221 In this study, we explored the neural representation of illusory faces and its relationship to human
222 behavior across a range of tasks. A key innovation of this project was the implementation of an unbiased
223 task to measure perceptual dissimilarity among faces, illusory faces, and matched objects within a
224 multidimensional space. This approach allowed us to confirm that human participants spontaneously
225 perceive illusory faces in ambient images of objects that coincidentally resemble faces. To gain a
226 comprehensive understanding of the behavioral dynamics, in separate experiments we asked
227 participants to; (1) rate the face-like appearance of each stimulus and (2) rapidly categorize each
228 stimulus as either a face or an object. As expected, these conventional behavioral tasks yielded
229 contrasting biases: participants rated illusory faces as more face-like than object-like in the ratings task
230 whereas participants categorized illusory faces as more object-like than face-like in the categorization
231 task. These findings underscore the considerable flexibility in the perception of illusory faces at the
232 behavioral level, which one might expect given their ambiguous and illusory nature. The next step was to
233 connect these behavioral patterns to time-resolved neural activity using multivariate analysis methods.

234

235 *Temporal Dynamics of Illusory Face Perception*

236 Using the same large set of images (i.e., 300 face and non-face stimuli), we employed EEG to first
237 replicate the finding that the neural representation of face pareidolia shifts from face-like to object-like
238 over time (Decramer et al., 2021; Rekow et al., 2022; Wardle et al., 2020). Then, by converging behavioral
239 and neural evidence, we discovered that the behavioral markers that captured the illusory face identity in
240 examples of face pareidolia (i.e., behavior in the triplet task and the ratings task) correlated with the
241 earliest evoked responses. In contrast, behavior in the face-object categorization task, which
242 emphasized the veridical object identity in examples of face pareidolia, correlated with later evoked
243 responses. This delay is somewhat paradoxical because the face-object categorization task was the only
244 speeded task. Rather than simply reflecting response speed, this temporal pattern suggests that
245 perception of face pareidolia unfolds through distinct computational stages, with early processes
246 supporting face detection and later stages mediating object recognition. One possibility is that face-
247 selective cortex is more excitable than object-selective regions. This would lead to the rapid propagation
248 of a neural signal reflecting the illusory face identity before knowledge about the object identity could be
249 extracted. Interestingly, while the correlations occur at different onsets, it is clear that the associations

250 between behavior and the neural time course were maintained over extended and overlapping periods of
251 time. Notably, early face-identity signals persist even after object-identity processes dominate,
252 suggesting the brain preserves initial interpretations rather than overwriting them. This provides critical
253 new insight the brain's capacity to build and maintain multiple independent representations in parallel.
254

255 *The Neural Time-Course Underlying the Spontaneous Perception of Face Pareidolia.*

256 Crucially, the results of the untargeted triplet odd-one-out task demonstrate that the facial features in
257 illusory objects were spontaneously perceived and used to make similarity judgements. While the
258 neural-behavior correlations that incorporate all 300 stimuli (Figure 3) were similar for the triplet and face
259 ratings task, likely reflecting broad category-level differences, Figure 4's exemplar specific analysis
260 shows that the triplet task uniquely captured information about semantically-matched object pairs. This
261 information was not captured by the explicit ratings or categorization behaviors. This demonstrates that
262 spontaneous dissimilarity judgements yield higher dimensionality than explicit ratings or categorization
263 behaviors with an enriched feature-specific signal capturing the similarity between object exemplars
264 from the same semantic categories (“nested object pairs”). The size of the stimulus set employed in our
265 study was important for detecting these subtle differences, enabling a nuanced understanding of how
266 targeted or untargeted task context influences the perception of ambiguous stimuli. This task-dependent
267 perceptual flexibility supports our previous work (Saurels et al., 2024; Stuart et al., 2025) showing that
268 behavior towards images containing two identities (i.e., objects with illusory faces) will differ depending
269 on the task at hand (for e.g., object-detection or face-detection).

270

271 *Behavioral Relevance as an Organizing Principle in the Visual Cortex*

272 Our findings align with theoretical frameworks that argue the organization of the visual cortex reflects
273 behavioral goals and stimulus affordances, not putative stimulus categories (Ritchie et al., 2024). Our
274 findings indicate that a single stimulus may evoke multiple neural representations that are maintained
275 over time. This capacity for building multiplexed representations would afford maximum behavioral
276 flexibility. For example, when we encounter face pareidolia, information about facial features is extracted
277 and becomes available for any task that makes the face relevant. But, shortly thereafter, information
278 about the object identity is computed for any task that makes the object relevant. It follows that,
279 because examples of face pareidolia have two distinct identities (i.e., a face and an object), possibly
280 represented by distinct mechanisms (Kanwisher, 2010; Sliwa & Freiwald, 2017; Taubert et al., 2015),

281 face pareidolia is a particularly useful tool for probing multiplexed representations. That said, multiplexed
282 representations would not necessarily be exclusive to face pareidolia because many if not all visual
283 objects could have latent identities, depending on a person's experience and task demands. For example,
284 when we see a banana, our brain might extract the visual features that make it look like a fruit and, thus,
285 build a representation similar to other fruits but our brain might also extract the visual features that make
286 a banana look 'tossable' and, thus, build a representation similar to other potential projectiles. This
287 perspective emphasizes the need to consider behavioral goals and stimulus affordances, but also their
288 flexibility, in understanding how the brain represents visual stimuli.

289

290 *Future Directions*

291 Future research could investigate individual differences in the propensity to perceive illusory faces in
292 specific exemplars (Taubert et al., 2023). Understanding these variations could provide deeper insights
293 into how neural responses shape perception and might reveal individual differences in the weighting of
294 early versus late processing stages. Such investigations could potentially uncover the neural basis for
295 individual variations in pareidolia susceptibility and their relationship to broader aspects of visual
296 processing.

297

298 *Theoretical Implications*

299 These findings make substantial contributions to our understanding of visual perception and neural
300 processing. The temporal dynamics of visual object recognition reveal a sophisticated system capable of
301 maintaining multiple interpretations simultaneously. The relationship between neural processing stages
302 and behavioral flexibility demonstrates how the brain can adaptively respond to different task demands
303 while maintaining access to multiple levels of representation. The maintenance of multiple
304 representations in visual perception suggests a more complex model of visual processing than previously
305 considered, while the integration of bottom-up visual features with top-down behavioral goals provides
306 insight into how the brain resolves perceptual ambiguity. Our results support a model where visual
307 perception emerges from the dynamic interplay between multiple processing stages, with task demands
308 modulating the relative contribution of each stage to behavioral outcomes. This framework provides a
309 more nuanced understanding of how the brain maintains and utilizes multiple levels of visual information
310 to support diverse perceptual judgments.

311

312 **Materials and Methods**

313 All code, stimuli and behavioral data will be available upon publication.

314

315 *Stimuli*

316 Stimulus images consisted of human faces, illusory faces and matched non-face objects. There were
317 300 stimuli: 100 exemplars each of human faces, illusory faces and matched objects (Figure 1A). The
318 same stimuli were used in all three behavioral tasks and the EEG experiment.

319

320 *Spontaneous dissimilarity task*

321 In this task, participants rated the similarity between the 300 experimental stimuli using a triplet odd-
322 one-out task (Grootswagers et al., 2024; Hebart et al., 2020). Participants were 338 undergraduate
323 students from the University of Sydney who participated in return for course credit. The experiments
324 were programmed in jsPsych (de Leeuw, 2015) and hosted on Pavlovia (Peirce et al., 2019). On each
325 trial, three experimental stimuli were presented simultaneously, and participants were asked to choose
326 the odd one out by clicking on the stimulus (Figure 1B). Stimuli were presented equidistant from fixation
327 in a triangle pattern. There were 300 trials in the experiment.

328

329 There was one main round of data collection with two subsequent rounds to ensure enough data
330 coverage across all stimuli. First, we collected judgements from N=328 participants using all 300
331 stimuli, with stimulus combinations chosen randomly on each trial. After collating the results, we
332 assessed which pairs of stimuli had never been presented together (67 pairs) and collected 5 more
333 participants by ensuring these stimulus pairs were included and excluding pairs with the highest
334 number of presentations (68 pairs). In a final round, we assessed which stimulus pairs had only
335 appeared once (372 pairs); we collected 5 more participants including these pairs and excluding pairs
336 presented the most (397 pairs with more than 13 presentations). In total, there were 101,397 trials,
337 with each of the 404,550 stimulus pairs presented at least once.

338

339 All trials from all participants were collated and the behavioral responses were used to construct a
340 representational dissimilarity matrix (RDM). For each trial, dissimilarity was calculated for the pairs of
341 stimuli (3 separate pairs for the 3 distinct stimuli). The stimulus chosen as the odd-one-out was coded
342 as dissimilar from each of the other two stimuli (values of 1), and the two other stimuli were coded as

343 similar (value of 0). The dissimilarity of each stimulus pair (e.g., face #1 vs illusory face #17) was
344 calculated as the mean dissimilarity value for all trials in which those two stimuli were presented
345 together. These mean values were used to construct a 300 x 300 RDM (Figure 2D).

346

347 *Face-like task*

348 Behavioral ratings were collected for the 300 stimuli. Participants were 20 undergraduates from the
349 University of Queensland (18 females, 2 males; median age 18.5 years, range 17-42 years) who
350 participated in return for course credit. Participants were shown each stimulus in turn, in random order,
351 and asked to “Rate how easily you can see a face in this image” on a scale of 0-10 (Figure 1C), as in
352 previous work (Taubert et al., 2023; Wardle et al., 2020, 2022). The experiment was programmed in
353 Qualtrics. Data from all participants were collated and the group mean face-like score was calculated
354 for each stimulus. A 300 x 300 dissimilarity matrix was constructed using Euclidean distance of face-
355 like scores for each pair of images (Figure 2E).

356

357 *Face-object categorization task*

358 In the final behavioral task, we used a forced-choice categorization task. Participants ($N = 23$; 17
359 females, 6 males; median age 22 years, range 18-30 years) were recruited from the University of
360 Queensland in return for payment in the form of gift cards (AUD\$20). They completed an experimental
361 session in the laboratory.

362

363 On each trial, a fixation cross was presented for 300ms, followed by a stimulus image, and finally a
364 Mondrian mask image was presented until the response. Participants were asked to press a button to
365 indicate if the stimulus was a face or an object. Stimuli were presented for 33.33 ms or 100 ms,
366 designed to tap into different stages of processing. There were 1200 trials in total, with two repeats of
367 each of the 300 stimuli per stimulus duration, presented in random order. Participants were given a
368 break every 300 trials. The experiment was programmed in Psychopy (Peirce et al., 2019) on a 1920 x
369 1080 VPixx monitor set at a refresh rate of 60 Hz. Stimuli and masks were presented at a size of 8 x 8
370 degrees of visual angle.

371

372 For each participant, the proportion of “face” categorization responses was calculated for each
373 stimulus and presentation condition. Data from all participants were then collated and the group mean

374 face-like score was calculated for each stimulus. There was no difference in the responses between
375 the two stimulus duration conditions ($t_{21} = .23$, $p = .817$) so we took the mean of both durations. A 300 x
376 300 dissimilarity matrix was then constructed using Euclidean distance of face categorization scores
377 for each pair of images (Figure 2E).

378

379

380 *EEG experiment*

381 Participants viewed stimuli that appeared centrally at fixation while their electroencephalography was
382 used to measure neural activity from the scalp. Participants were 20 adults recruited from the University
383 of Queensland (16 females, 4 males; median age 22.5 years, range 18-30 years) and were compensated
384 for their time at a rate of AUD\$20 per hour. Informed consent was obtained from all participants. All
385 participants reported normal or corrected-to-normal vision.

386

387 Stimuli were presented using Psychopy (Peirce et al., 2019) at approximately 4×4 degrees of visual
388 angle on a gamma-corrected LCD monitor (VIEWPixx 3D, VPixx Technologies; 1920 x 1080 pixels, 22.5-
389 inch, 120 Hz refresh rate). Images were presented in sequences of 150 stimuli such that two adjacent
390 sequences contained each of the 300 experimental stimuli once, in random order. Every sequence
391 began with a fixation dot for 500 ms, then stimuli were presented one after another for 133.33 ms with
392 an inter-stimulus interval of 133.33 ms (i.e., images presentation at a rate of 3.75 Hz). Across the
393 experiment, there were 70 sequences totaling 10,500 trials, consisting of 35 repeats for each of the 300
394 stimuli.

395

396 During the experimental session, participants were asked to maintain fixation on the dot that appeared
397 in the center of the screen in black, detect when it turned red (Figure 1B) and indicate detection by
398 button press. This task was designed to be orthogonal and irrelevant to the stimuli. The rapid stimulus
399 presentation, random image sequences and orthogonal task reduced the likelihood of participants
400 moving their eyes in a stimulus-specific manner.

401

402 *EEG recording and preprocessing*

403 EEG data were continuously recorded from a 64-electrode BioSemi system, arranged in the
404 international 10–20 system for electrode placement (Oostenveld & Praamstra, 2001), digitized at a

405 sample rate of 1024 Hz. The EEGLAB toolbox (Delorme & Makeig, 2004) was used to preprocess the
406 data offline. First, we re-referenced to channel Cz, then filtered the data using a Hamming windowed
407 sinc FIR filter with high pass of 0.1Hz and lowpass of 100Hz as in our previous work (Grootswagers et
408 al., 2019; Robinson et al., 2019). Following these steps, noisy electrodes were identified using joint
409 probability and were reconstructed using spherical interpolation if they exceeded 5 standard deviations
410 from the average (mean number interpolated = .25, min = 1, max = 3). A common average reference was
411 then applied, and data were downsampled to 256 Hz. Finally, epochs were created for each stimulus
412 presentation from [-100 to 1000ms] relative to stimulus onset, and baseline corrected. No other pre-
413 processing or data cleaning was performed.

414

415 *Neural decoding*

416 To investigate how the perception of face pareidolia unfolds over time, we assessed the neural
417 representations of human face, illusory face and matched non-face object stimuli (Figure 1A).
418 Multivariate pattern analysis, or neural decoding, was applied to the time-resolved EEG data to
419 discriminate how different stimuli evoked different patterns of neural activity over the scalp (Carlson et
420 al., 2020; Robinson et al., 2023). For each time point (3.90 ms time resolution) and participant, we
421 assessed stimulus-specific representations by training a classifier to discriminate between neural
422 activity associated with two experimental stimuli and testing on held out data for the same stimuli.
423 Decoding was implemented using the CoSMoMVPA toolbox (Oosterhof et al., 2016). Data were pooled
424 across the 64 EEG sensors, and we tested the ability of a linear discriminant analysis (LDA) classifier to
425 discriminate between the patterns of neural responses associated with each stimulus. A 35-fold cross-
426 validation procedure was used, with each fold containing 2 independent trial sequences (one repeat of
427 each stimulus). All pairs of combinations for the 300 stimuli (e.g., humanface1 vs illusoryface2,
428 illusoryface87 vs matchedobject4) were decoded, resulting in 44,850 unique contrasts across time per
429 participant. Classifier accuracy was calculated as the mean proportion of correct classifier predictions
430 across all folds. Above chance group mean decoding accuracy (above 50%) was considered evidence
431 of stimulus information in the neural signals.

432

433 *Representational similarity analyses*

434 To investigate the relationship in the structure of stimulus representations between the neural
435 responses measured via EEG and perception measures via behavioral tasks, we used representational

436 similarity analyses (RSA) (Kriegeskorte et al., 2008). RSA involves a neural-behavior comparison that is
437 abstracted away from task-specific or methodology-specific responses, instead focusing on the
438 relationships between stimulus representations. This set of analyses allowed us to assess the content
439 of information within neural representations that relates to behavior.

440

441 Using the neural and behavioral results, we constructed representational dissimilarity matrices (RDMs),
442 which quantified the similarity between each stimulus. Each of these RDM models was a 300×300
443 matrix of dissimilarity for each of the 300 stimuli with each other stimulus, using the relevant neural or
444 behavioral measure. The RDMs were symmetrical across the diagonal, with 44,850 unique values.

445

446 For each behavioral task, a dissimilarity matrix was constructed based on the difference in mean
447 behavioral responses across stimulus pairs (Figure 2A). As a comparison, we constructed three face-
448 object category models: a face model that codes illusory faces as faces, an object model that codes
449 illusory faces as objects, and an illusory face model that codes illusory faces as a separate third
450 category from faces and objects (Figure 2B). All behavioral and category models were significantly
451 correlated ($\rho > .097$, $p < .001$).

452

453 Neural RDMs used decoding accuracy for each pair of stimuli at each time point (3.90 ms temporal
454 resolution). Separate 300×300 neural RDMs were constructed for each time point and participant,
455 where each cell contained the mean decoding accuracy between two stimuli. The behavioral RDMs
456 were based on the group mean dissimilarity scores from the three behavioral experiments. We also
457 constructed three additional stimulus models based on the stimulus category: the face model, which
458 classed illusory faces and faces as distinct from objects; the object model, which classed illusory faces
459 and objects as distinct from human faces, and the illusory face model, which classed illusory faces as
460 distinct from both human faces and objects.

461

462 Using RSA, we investigated how neural representations related to behavioral judgements. Neural RDMs
463 per participant were correlated with each behavioral RDM using Spearman correlation to assess
464 similarity of the lower diagonals of the RDMs (i.e., the unique pairwise values), for every time point. This
465 allowed us to assess how neural information might inform overall perception. Correlations were
466 performed for each EEG participant separately and the mean was calculated across the group.

467

468 *Statistical testing*

469 To assess neural-behavior correlations, we used Bayesian statistics to determine the evidence for the
470 alternative relative to the null hypotheses (Dienes, 2011, 2016; Jeffreys, 1961; Rouder et al., 2009;
471 Wagenmakers, 2007). For decoding analyses, the alternative hypothesis of above-chance (50%)
472 decoding was tested. For correlation analyses, the alternative hypotheses of above- and below- zero
473 correlations were tested. We used the ‘BayesFactor’ package in R (Morey et al., 2018). Bayes Factors
474 were calculated using a JZS prior, centered around chance decoding of 50% (Rouder et al., 2009) with
475 default scale factor of 0.707, meaning that for the alternative hypotheses of above- and below- chance
476 decoding, we expected to see 50% of parameter values falling within -.707 and .707 standard
477 deviations from chance (Jeffreys, 1961; Rouder et al., 2009; Wetzels & Wagenmakers, 2012; Zellner &
478 Siow, 1980). A null interval was specified as a range of effect sizes between -0.5 to 0.5 (Teichmann et
479 al., 2022).

480 A Bayes Factor (BF) is the probability of the data under the alternative hypothesis relative to the null
481 hypothesis. We consider $BF > 3$ as evidence for the alternative hypothesis (above-chance decoding and
482 reliable correlations). We interpret $BF < 1/3$ as evidence in favor of the null hypothesis (Jeffreys, 1961;
483 Wetzels et al., 2011).

484

485 **References**

- 486 Afraz, S.-R., Kiani, R., & Esteky, H. (2006). Microstimulation of inferotemporal cortex influences face
487 categorization. *Nature*, 442(7103), 692–695. <https://doi.org/10.1038/nature04982>
- 488 Azadi, R., Lopez, E., Taubert, J., Patterson, A., & Afraz, A. (2023). The causal link between neural activity
489 in inferotemporal cortex and free viewing eye movements. *Journal of Vision*, 23(9), 5739.
490 <https://doi.org/10.1167/jov.23.9.5739>
- 491 Carlson, T. A., Grootswagers, T., & Robinson, A. K. (2020). *An Introduction to Time-Resolved Decoding
492 Analysis for M/EEG*. <https://doi.org/10.7551/mitpress/11442.003.0075>
- 493 de Leeuw, J. R. (2015). jsPsych: A JavaScript library for creating behavioral experiments in a Web
494 browser. *Behavior Research Methods*, 47(1), 1–12. <https://doi.org/10.3758/s13428-014-0458-y>
- 495 Decramer, T., Premereur, E., Caprara, I., Theys, T., & Janssen, P. (2021). Temporal dynamics of neural
496 activity in macaque frontal cortex assessed with large-scale recordings. *NeuroImage*, 236,
497 118088. <https://doi.org/10.1016/j.neuroimage.2021.118088>
- 498 Delorme, A., & Makeig, S. (2004). EEGLAB: An open source toolbox for analysis of single-trial EEG
499 dynamics including independent component analysis. *Journal of Neuroscience Methods*, 134,
500 9–21. <https://doi.org/10.1016/j.jneumeth.2003.10.009>
- 501 Dienes, Z. (2011). Bayesian Versus Orthodox Statistics: Which Side Are You On? *Perspectives on
502 Psychological Science*, 6(3), 274–290. <https://doi.org/10.1177/1745691611406920>
- 503 Dienes, Z. (2016). How Bayes factors change scientific practice. *Journal of Mathematical Psychology*,
504 72, 78–89. <https://doi.org/10.1016/j.jmp.2015.10.003>
- 505 Dy, T., Wa, F., Rb, T., & Ms, L. (2006). A cortical region consisting entirely of face-selective cells.
506 *Science (New York, N.Y.)*, 311(5761). <https://doi.org/10.1126/science.1119983>

- 508 Epihova, G., Cook, R., & Andrews, T. J. (2022). Recognition of pareidolic objects in developmental
509 prosopagnosic and neurotypical individuals. *Cortex*, 153, 21–31.
510 <https://doi.org/10.1016/j.cortex.2022.04.011>
- 511 Grootswagers, T., Robinson, A. K., & Carlson, T. A. (2019). The representational dynamics of visual
512 objects in rapid serial visual processing streams. *NeuroImage*, 188, gro.
513 <https://doi.org/10.1016/j.neuroimage.2018.12.046>
- 514 Grootswagers, T., Robinson, A. K., Shatek, S. M., & Carlson, T. A. (2024). Mapping the dynamics of visual
515 feature coding: Insights into perception and integration. *PLOS Computational Biology*, 20(1),
516 e1011760. <https://doi.org/10.1371/journal.pcbi.1011760>
- 517 Hebart, M. N., Zheng, C. Y., Pereira, F., & Baker, C. I. (2020). Revealing the multidimensional mental
518 representations of natural objects underlying human similarity judgements. *Nature Human
519 Behaviour*, 4(11), Article 11. <https://doi.org/10.1038/s41562-020-00951-3>
- 520 Jeffreys, H. (1961). *Theory of probability* (Third). Oxford University Press.
- 521 Kanwisher, N. (2000). Domain specificity in face perception. *Nature Neuroscience*, 3(8), 759–763.
522 <https://doi.org/10.1038/77664>
- 523 Kanwisher, N. (2010). Functional specificity in the human brain: A window into the functional
524 architecture of the mind. *Proceedings of the National Academy of Sciences*, 107(25), 11163–
525 11170. <https://doi.org/10.1073/pnas.1005062107>
- 526 Kanwisher, N., McDermott, J., & Chun, M. M. (1997). The Fusiform Face Area: A Module in Human
527 Extrastriate Cortex Specialized for Face Perception. *Journal of Neuroscience*, 17(11), 4302–
528 4311.

- 529 Keys, R. T., Taubert, J., & Wardle, S. G. (2021). A visual search advantage for illusory faces in objects.
- 530 *Attention, Perception, & Psychophysics*, 83(5), 1942–1953. <https://doi.org/10.3758/s13414-021-02267-4>
- 531
- 532 Kriegeskorte, N., Mur, M., & Bandettini, P. a. (2008). Representational similarity analysis—Connecting
- 533 the branches of systems neuroscience. *Frontiers in Systems Neuroscience*, 2(November), 4–4.
- 534 <https://doi.org/10.3389/neuro.06.004.2008>
- 535 Liu, J., Li, J., Feng, L., Li, L., Tian, J., & Lee, K. (2014). Seeing Jesus in toast: Neural and behavioral
- 536 correlates of face pareidolia. *Cortex; a Journal Devoted to the Study of the Nervous System and*
- 537 *Behavior*, 53, 60–77. <https://doi.org/10.1016/j.cortex.2014.01.013>
- 538 Meng, M., Cherian, T., Singal, G., & Sinha, P. (2012). Lateralization of face processing in the human
- 539 brain. *Proceedings of the Royal Society B: Biological Sciences*, 279(1735), 2052–2061.
- 540 <https://doi.org/10.1098/rspb.2011.1784>
- 541 Morey, R. D., Rouder, J. N., Jamil, T., Urbanek, S., Forner, K., & Ly, A. (2018, May 19). *Package*
- 542 “*BayesFactor*.” [https://cran.r-project.org/web/packages/ BayesFactor/ BayesFactor.pdf](https://cran.r-project.org/web/packages/BayesFactor/ BayesFactor.pdf)
- 543 Omer, Y., Sapir, R., Hatuka, Y., & Yovel, G. (2019). What Is a Face? Critical Features for Face Detection.
- 544 *Perception*, 48, 030100661983873. <https://doi.org/10.1177/0301006619838734>
- 545 Oostenveld, R., & Praamstra, P. (2001). The five percent electrode system for high-resolution EEG and
- 546 ERP measurements. *Clinical Neurophysiology*, 112(4), 713–719.
- 547 [https://doi.org/10.1016/S1388-2457\(00\)00527-7](https://doi.org/10.1016/S1388-2457(00)00527-7)
- 548 Oosterhof, N. N., Connolly, A. C., & Haxby, J. V. (2016). CoSMoMVPA: Multi-Modal Multivariate Pattern
- 549 Analysis of Neuroimaging Data in Matlab/GNU Octave. *Frontiers in Neuroinformatics*, 10.
- 550 <https://doi.org/10.3389/fninf.2016.00027>

- 551 Peirce, J., Gray, J. R., Simpson, S., MacAskill, M., Höchenberger, R., Sogo, H., Kastman, E., & Lindeløv, J.
- 552 K. (2019). PsychoPy2: Experiments in behavior made easy. *Behavior Research Methods*, 51(1),
- 553 195–203. <https://doi.org/10.3758/s13428-018-01193-y>
- 554 Puce, A., Allison, T., Asgari, M., Gore, J. C., & McCarthy, G. (1996). Differential Sensitivity of Human
- 555 Visual Cortex to Faces, Letterstrings, and Textures: A Functional Magnetic Resonance Imaging
- 556 Study. *The Journal of Neuroscience*, 16(16), 5205. <https://doi.org/10.1523/JNEUROSCI.16-16-05205.1996>
- 557
- 558 Quian Quiroga, R., Boscaglia, M., Jonas, J., Rey, H. G., Yan, X., Maillard, L., Colnat-Coulbois, S.,
- 559 Koessler, L., & Rossion, B. (2023). Single neuron responses underlying face recognition in the
- 560 human midfusiform face-selective cortex. *Nature Communications*, 14(1), 5661.
- 561 <https://doi.org/10.1038/s41467-023-41323-5>
- 562 Rekow, D., Baudouin, J.-Y., Brochard, R., Rossion, B., & Leleu, A. (2022). Rapid neural categorization of
- 563 facelike objects predicts the perceptual awareness of a face (face pareidolia). *Cognition*, 222,
- 564 105016. <https://doi.org/10.1016/j.cognition.2022.105016>
- 565 Ritchie, J. B., Wardle, S. G., Vaziri-Pashkam, M., Kravitz, D. J., & Baker, C. I. (2024). *Rethinking category-*
- 566 *selectivity in human visual cortex* (arXiv:2411.08251). arXiv.
- 567 <https://doi.org/10.48550/arXiv.2411.08251>
- 568 Robinson, A. K., Grootswagers, T., & Carlson, T. A. (2019). The influence of image masking on object
- 569 representations during rapid serial visual presentation. *NeuroImage*, 197, 224–231.
- 570 <https://doi.org/10.1016/j.neuroimage.2019.04.050>
- 571 Robinson, A. K., Quek, G. L., & Carlson, T. A. (2023). Visual Representations: Insights from Neural
- 572 Decoding. *Annual Review of Vision Science*, 9(1), 313–335. <https://doi.org/10.1146/annurev-vision-100120-025301>
- 573

- 574 Romagnano, V., Kubon, J., Sokolov, A. N., Fallgatter, A. J., Braun, C., & Pavlova, M. A. (2024). Dynamic
575 brain communication underwriting face pareidolia. *Proceedings of the National Academy of
576 Sciences*, 121(16), e2401196121. <https://doi.org/10.1073/pnas.2401196121>
- 577 Rossion, B., Hanseeuw, B., & Dricot, L. (2012). Defining face perception areas in the human brain: A
578 large-scale factorial fMRI face localizer analysis. *Brain and Cognition*, 79(2), 138–157.
579 <https://doi.org/10.1016/j.bandc.2012.01.001>
- 580 Rouder, J. N., Speckman, P. L., Sun, D., Morey, R. D., & Iverson, G. (2009). Bayesian t tests for accepting
581 and rejecting the null hypothesis. *Psychon Bull Rev*, 16(2), 225–237.
582 <https://doi.org/10.3758/PBR.16.2.225>
- 583 Sadagopan, S., Zarco, W., & Freiwald, W. A. (2017). A causal relationship between face-patch activity
584 and face-detection behavior. *eLife*, 6, e18558. <https://doi.org/10.7554/eLife.18558>
- 585 Saurels, B. W., Peluso, N., & Taubert, J. (2024). A behavioral advantage for the face pareidolia illusion in
586 peripheral vision. *Scientific Reports*, 14(1), 10040. <https://doi.org/10.1038/s41598-024-60892-z>
- 587 z
- 588 Sliwa, J., & Freiwald, W. A. (2017). A dedicated network for social interaction processing in the primate
589 brain. *Science*, 356(6339), 745–749. <https://doi.org/10.1126/science.aam6383>
- 590 Stuart, G., Saurels, B. W., Robinson, A., & Taubert, J. (2025). One object with two identities: The rapid
591 detection of face pareidolia in face and food detection tasks. *Journal of Experimental
592 Psychology: Human Perception and Performance*. <https://doi.org/10.31234/osf.io/5983j>
- 593 Taubert, J., Van Belle, G., Vanduffel, W., Rossion, B., & Vogels, R. (2015). The effect of face inversion for
594 neurons inside and outside fMRI-defined face-selective cortical regions. *Journal of
595 Neurophysiology*, 113(5), 1644–1655. <https://doi.org/10.1152/jn.00700.2014>

- 596 Taubert, J., Wally, S., & Dixson, B. J. (2023). Preliminary evidence of an increased susceptibility to face
597 pareidolia in postpartum women. *Biology Letters*, 19(9), 20230126.
598 <https://doi.org/10.1098/rsbl.2023.0126>
- 599 Taubert, J., Wardle, S. G., Flessert, M., Leopold, D. A., & Ungerleider, L. G. (2017). Face Pareidolia in the
600 Rhesus Monkey. *Current Biology: CB*, 27(16), 2505-2509.e2.
601 <https://doi.org/10.1016/j.cub.2017.06.075>
- 602 Taubert, J., Wardle, S. G., Tardiff, C. T., Patterson, A., Yu, D., & Baker, C. I. (2022). Clutter Substantially
603 Reduces Selectivity for Peripheral Faces in the Macaque Brain. *Journal of Neuroscience*, 42(35),
604 6739–6750. <https://doi.org/10.1523/JNEUROSCI.0232-22.2022>
- 605 Teichmann, L., Moerel, D., Baker, C., & Grootswagers, T. (2022). An Empirically Driven Guide on Using
606 Bayes Factors for M/EEG Decoding. *Aperture Neuro*, 2, 1–10.
607 <https://doi.org/10.52294/ApertureNeuro.2022.2.MAOC6465>
- 608 Uchiyama, M., Nishio, Y., Yokoi, K., Hirayama, K., Imamura, T., Shimomura, T., & Mori, E. (2012).
609 Pareidolias: Complex visual illusions in dementia with Lewy bodies. *Brain: A Journal of
610 Neurology*, 135(Pt 8), 2458–2469. <https://doi.org/10.1093/brain/aws126>
- 611 Wagenmakers, E. (2007). A practical solution to the pervasive problems of p values. *Psychonomic
612 Bulletin and Review*, 14(5), 779–804. <https://doi.org/10.3758/BF03194105>
- 613 Wardle, S. G., Paranjape, S., Taubert, J., & Baker, C. I. (2022). Illusory faces are more likely to be
614 perceived as male than female. *Proceedings of the National Academy of Sciences*, 119(5),
615 e2117413119. <https://doi.org/10.1073/pnas.2117413119>
- 616 Wardle, S. G., Taubert, J., Teichmann, L., & Baker, C. I. (2020). Rapid and dynamic processing of face
617 pareidolia in the human brain. *Nature Communications*, 11(1), Article 1.
618 <https://doi.org/10.1038/s41467-020-18325-8>

- 619 Wetzels, R., Matzke, D., Lee, M. D., Rouder, J. N., Iverson, G. J., & Wagenmakers, E. J. (2011). Statistical
620 evidence in experimental psychology: An empirical comparison using 855 t tests. *Perspectives*
621 *on Psychological Science*, 6(3), 291–298. <https://doi.org/10.1177/1745691611406923>
- 622 Wetzels, R., & Wagenmakers, E.-J. (2012). A default Bayesian hypothesis test for correlations and
623 partial correlations. *Psychonomic Bulletin & Review*, 19(6), 1057–1064.
624 <https://doi.org/10.3758/s13423-012-0295-x>
- 625 Zellner, A., & Siow, A. (1980). Posterior odds ratios for selected regression hypotheses. *Trabajos de*
626 *Estadistica Y de Investigacion Operativa*, 31(1), 585–603. <https://doi.org/10.1007/BF02888369>
- 627